APPLICATIONS OF 3D QUANTUM TRANSPORT SIMULATIONS

D. Z.-Y. Ting, S. K. Kirby, and T. C. McGill
Thomas J. Watson, Sr., Laboratory of Applied Physics
California Institute of Technology
Pasadena, California 91125, U.S.A.

Abstract

Quantum transport in low dimensional nanostructures is examined with an exactly solvable real-space three-dimensional supercell model. Applications to the following examples are discussed : (1) finite length quantum wires, (2) alloy clustering effects in single barrier tunnel structures, and (3) quantum dot arrays.

I. INTRODUCTION

We developed a flexible 3D model aimed at exploring issues relevant to quantum transport in nanostructures, including effects of reduced dimensionality and structural inhomogeneities. Using our method we have demonstrated that interfacial inhomogeneities in double barrier resonant tunneling diodes can induce lateral localization of wave functions [1]; strongly attractive impurities can produce additional transmission resonances [2]; and surface roughness in quantum dots can cause large fluctuations in transmission characteristics [3]. In this paper, we examine transport through single barrier tunnel structures with alloy clustering, and relate it to transport through quantum wires. We also examine transport through quantum dot arrays.

II. METHOD

We use a planar supercell tight-binding Hamiltonian and specify the active region of a structure as a stack of N_z layers perpendicular to the z-direction, with each layer containing a periodic array of rectangular planar supercells of $N_x \times N_y$ sites. Within each planar supercell, the potential assumes lateral variations as dictated by device geometry. Our method obtains exact scattering plane wave solutions [1, 2], subject to supercell periodic boundary conditions in the x- and y-directions, and open boundary conditions in the z-direction. Our method requires accurate and efficient solutions of large sparse linear systems, which is achieved using the quasi-minimal residual method [4].

III. APPLICATIONS

We apply our method to the following examples : (1) finite length quantum wires, (2) quantum dot arrays, and (3) clustering effects in alloy barriers. In all three cases, the band edge and effective mass values for well- and barrier-type materials used are : $E_C^W = 0$ eV, $m_W^* = 0.0673\ m_0$, $E_C^B = 1.05$ eV, $m_B^* = 0.1248\ m_0$; the choice of these material parameters nominally correspond GaAs and AlAs, respectively.

1. Finite Length Quantum Wires

We first examine finite-length quantum wire electron waveguides. We consider GaAs quantum wires surrounded on the sides by AlAs walls, and the ends by GaAs electrodes. The wires have

40Å×40Å cross-section, and wire lengths ranging from 50Å to 800Å. We study the dependence of quantum wire transmission properties on channel length. The transmission spectra in Fig. 1 show that as the quantum wire channel length increases, the number of transmission resonances increases, corresponding to an increasing number of modes in the wire. Note that in all the spectra shown, transmission coefficient tends to be quite small for electron energy below ≈ 0.3 eV. In Fig. 2 we plot the same set of transmission spectra on a semilogarithmic scale to reveal the sub-threshold behavior. We see that there is a cutoff energy (analogues to cutoff frequency in metallic waveguides for electromagnetic waves), and that the cutoff becomes sharper as the channel length increases.

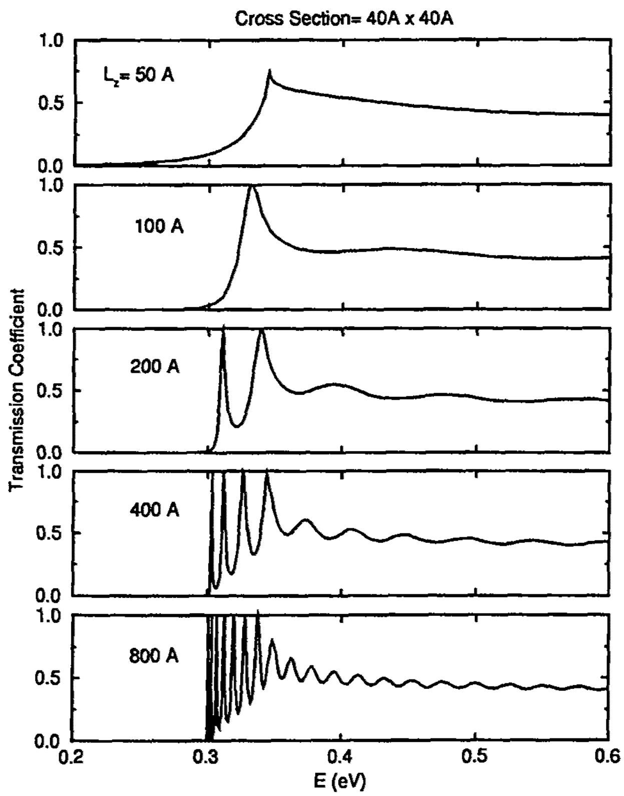

Fig. 1. Transmission coefficients for a set of quantum wire structures with various channel lengths.

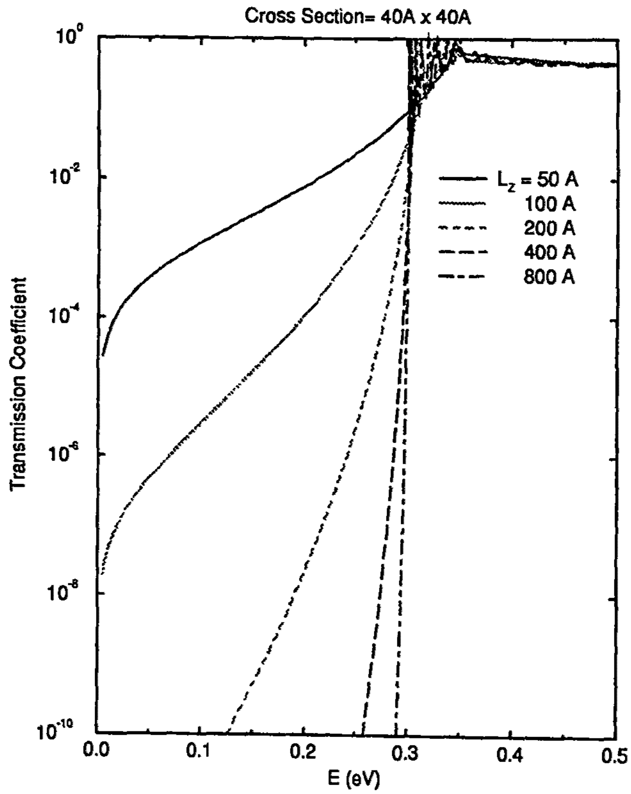

Fig. 2. Transmission coefficients for structures similar to those in Fig. 1, shown in semilog scale.

2. Alloy Clustering Effects in Single Barrier Tunnel Structures

We next consider tunneling characteristics of single barrier GaAs/$Al_{0.5}Ga_{0.5}As$ structures of varying thickness. It can be demonstrated that for totally random alloy configurations, the virtual crystal approximation yields transmission characteristics which are in agreement with supercell calculation results. However, if we allow the AlAs sites (equivalently, the GaAs sites) in the barrier to cluster, then tunneling characteristics can change significantly. Fig. 3 shows the transmission spectra for 50Å, 100Å, and 200Å thick barriers, with cluster size (average in-plane cluster "diameter") of $\lambda =$ 65Å. Note that the spectra show typical single barrier tunneling characteristics below a threshold energy (≈ 0.18 eV). Above the threshold, the even thick barriers becomes somewhat transparent. The threshold energy decreases as cluster size increase, as depicted in Fig. 4. The above-threshold behavior can be explained in terms of short wavelength electrons penetrating through the barrier via channels formed by GaAs clusters. The transport mechanism is analogous to that in finite length quantum wires; a comparison between Fig. 3 and Figs. 1 & 2 shows qualitative similarities.

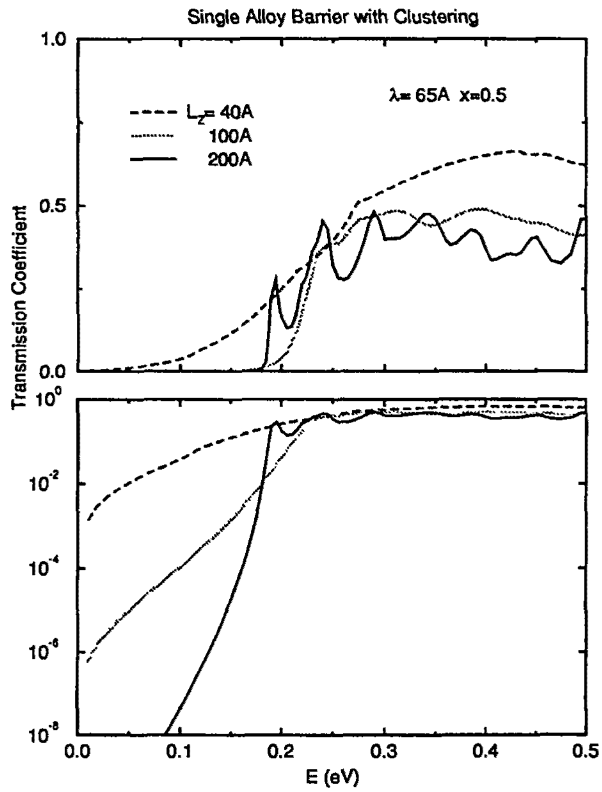

Fig. 3. Transmission coefficients a set of single alloy barrier tunnel structures with different barrier thickness.

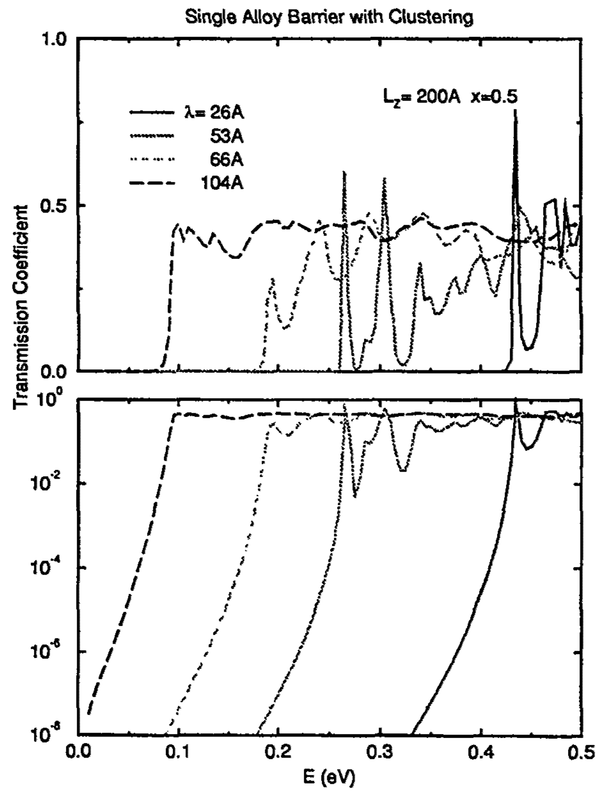

Fig. 4. Transmission coefficients for a set of single alloy barrier tunnel structures with varying degrees of clustering.

3. Quantum Dot Arrays

In the final example we study transmission properties of quantum dot arrays, which consist of (40 Å)^3 dots arranged in a 2D square lattice, embedded between a pair of 20 Å barrier layers. We consider the following three cases as illustrated in Fig. 5 : (1) isolated dots, where the dots are separated laterally by 40 Å barriers, (2) interacting dots, where the interdot barriers are 10 Å wide, and, for comparison, (3) the limiting case of zero interdot separation, which is simply a double barrier structure. Transmission spectra for these structures with various values of lateral incoming plane wave momentum are shown in Fig. 6. While all the spectra show resonances corresponding to the quantized levels in the quantum dots (quantum well), they differ significantly in their $\mathbf{k}_{\|}$ dependence. The double barrier structure shows $\mathbf{k}_{\|}$ dispersion similar to bulk GaAs, as expected. The array of isolated dots shows no $\mathbf{k}_{\|}$ dispersion, due to 0D quantum confinement. The array of interacting dots can be considered as a 2D solid composed of interacting artificial atoms, forming its own band structure differing significantly from that of bulk GaAs. This is quite evident in Fig. 6. We note in particular that the splitting of the $n = 2$ peak due to the interaction of p-like bands.

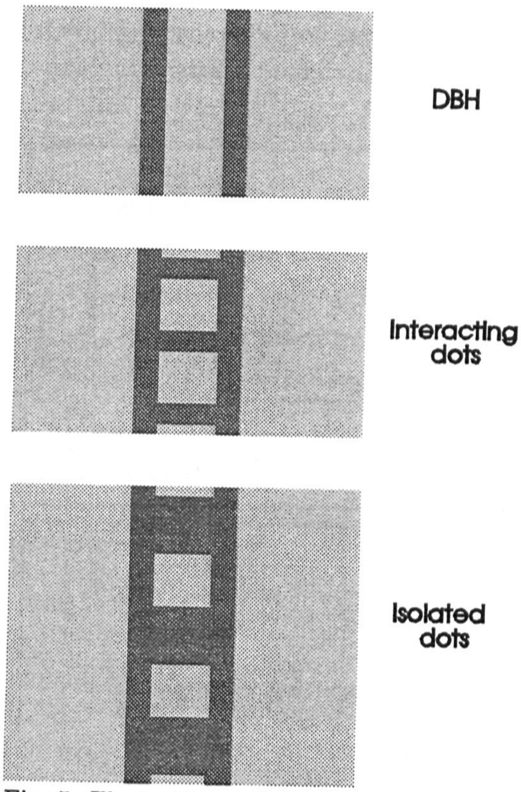

Fig. 5. Illustrations of closely-spaced and isolated quantum dot arrays. A double barrier structure is included for comparison.

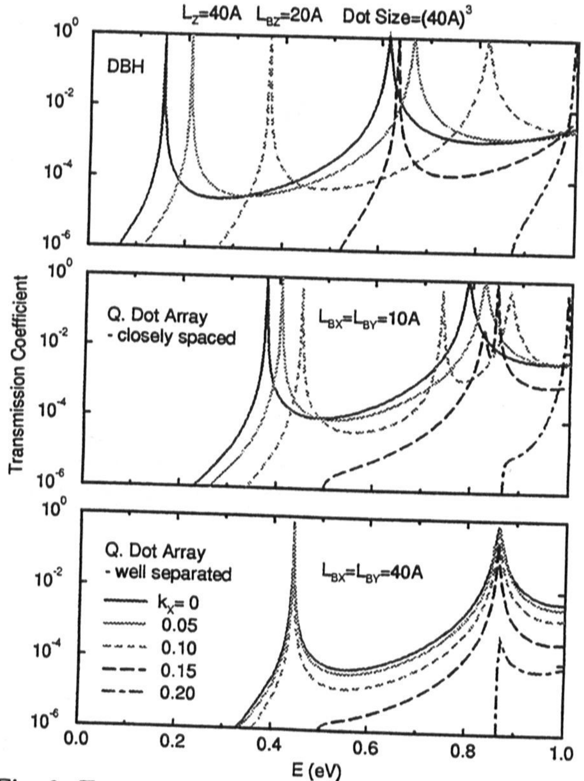

Fig. 6. Transmission coefficients a structures illustrated in Fig. 5.

IV. SUMMARY

We examine transport through single barrier tunnel structures with alloy clustering, and relate it to transport through quantum wires. This demonstrates that structural imperfections can not only produce additional scattering processes in a perturbative sense, but also alter quantized electronic states, leading to substantially modified transport properties. We also studied arrays of mesoscopic devices, where transport properties are strongly influenced by coherence among closely-spaced device structures.

Acknowledgment

The authors would like to thank Eric Van de Velde, R. K. Smith, and W. R. Frensley for helpful discussions. This work was supported by the U. S. Office of Naval Research (ONR) under Grant No. N00014-89-J-1141.

References

[1] D. Z.-Y. Ting, S. K. Kirby, and T. C. McGill, Appl. Phys. Lett. **64**, 2004 (1994).

[2] S. K. Kirby, D. Z.-Y. Ting, and T. C. McGill, Phys. Rev. B **48**, 15237 (1993).

[3] S. K. Kirby, D. Z.-Y. Ting, and T. C. McGill, To be published in Phys. Rev. B.

[4] R. W. Freund and N. M. Nachtigal, Numer. Math. **60**(3), 315 (1991). Technical Report 90.51, RIACS, NASA Ames Research Center, Dec. 1989.